Materials Research, Vol. 5, No. 3, 231-241, 2002.

Stochastic Effects in Microstructure

M.E. Glicksman, K.G. Wang* and P. Crawford

Materials Science and Engineering Department,
Rensselaer Polytechnic Institute, Troy, NY 12180-3590

Received: September 27, 2001; Revised: July 10, 2002

We are currently studying microstructural responses to diffusion-limited coarsening in two-phase materials. A mathematical solution to late-stage multiparticle diffusion in finite systems is formulated with account taken of particle-particle interactions and their microstructural correlations, or "locales". The transition from finite system behavior to that for an infinite microstructure is established analytically. Large-scale simulations of late-stage phase coarsening dynamics show increased fluctuations with increasing volume fraction, V_v, of the mean flux entering or leaving particles of a given size class. Fluctuations about the mean flux were found to depend on the scaled particle size, R/<R>, where R is the radius of a particle and <R> is the radius of the dispersoid averaged over the population within the microstructure. Specifically, small (shrinking) particles tend to display weak fluctuations about their mean flux, whereas particles of average, or above average size, exhibit strong fluctuations. Remarkably, even in cases of microstructures with a relatively small volume fraction ($V_v \approx 10^{-4}$), the particle size distribution is broader than that for the well-known Lifshitz-Slyozov limit predicted at zero volume fraction. The simulation results reported here provide some additional surprising insights into the effect of diffusion interactions and stochastic effects during evolution of a microstructure, as it approaches its thermodynamic end-state.

Keywords: *microstructural evolution, coarsening processes, simulation, stochastic effect*

1. Introduction

Phase coarsening is a spontaneous kinetic process in late-stage microstructural evolution that leads to the decrease in the interfacial energy of two-phase systems. The biphase system consists typically of individual dispersed domains, crystallites, or particles, distributed more-or-less at random through another contiguous matrix phase. During phase coarsening, the transport of atoms via lattice diffusion proceeds through the intervening matrix phase from solute sources at particle-matrix interfaces with high mean curvature towards solute sinks at particle-matrix interfaces with low mean curvature. Typically, in such systems, larger particles tend to grow at the expense of small particles. Over time, as the smallest particles dissolve, the "competitive" multiparticle diffusion process among particles results in an increase in the average size of their population, and in a concomitant decrease in their number. When matrix diffusion is the rate-limiting atomic transport process, the average particle size increases with sub-linear kinetics (cube-root of time) and the particle number density decreases reciprocally with time. These kinetic "signatures", observed in many aging microstructures, are so robust and fundamental as to be virtually independent of the physical model.

The particle size and microstructure representative of many cast and liquid-phase sintered alloys are known to depend on similar phase coarsening processes. Moreover, the physical and chemical properties of these materials, such as their strength, toughness, ductility, electrical conductivity, and corrosion resistance all depend on the material's average particle size and particle size distribution (PSD). Understanding and controlling microstructures in two-phase systems are materials science topics with broad technological implications. Indeed, predicting microstructure evolution in general remains a cornerstone of modern materials science.

Predicting microstructure evolution quantitatively from first principles has an interesting 40-year history. Todes[1] published the seminal paper on formulating the phase coarsening dynamics. However, the initial theory of capillary-

*e-mail: wangk2@rpi.edu

mediated phase coarsening was completed by Lifshitz and Slyozov[2], and, then independently, by Wagner[3]. These theories collectively are often referred to as "LSW theory". A major assumption in LSW theory is that particles with equal size experience the same time-rate of change of their volume or mass. LSW theory predicts that (1) the average volume (or cube of the radius) of the particle population increases *linearly* with time-a fact borne out by numerous careful experiments in many different systems; and (2) that the PSD predicted from LSW theory is self-affine, which implies that the particle patterns at later times appear statistically similar to those observed at earlier times, apart from a uniform global increase of size scale. However, the rate constant controlling the kinetics of the evolving length scales, and the PSD predicted from LSW theory, both disagree with the preponderant body of quantitative experiments on coarsening microstructures[4,5].

LSW theory is a "limit law", insofar as it applies strictly to microstructures with *zero* volume fraction of dispersoid phase. The predicted PSD and coarsening rate based on LSW theory therefore ignores all interactions occurring among particles. For any volume fraction of the dispersoid phase, other than *zero*, the particles would have neighbors positioned at finite distances. Interactions among them clearly become possible. Recently, Glicksman, Wang and Marsh[6] reviewed the interaction effects among dispersed particles, and described how such interactions influence the PSD and the kinetics of coarsening. Another source of error in the predicted PSD and coarsening rates at finite volume fractions is that caused by influences of the unique microstructural environment encountered by each particle – i.e., its "locale". Locale differences are ignored when adhering to the tenets of mean-field theory, whereas, in fact, it is known that particles of the same size located at different positions in a microstructure may exhibit different growth rates.

The subject of stochastics in late-stage phase coarsening, although still in an early stage of development, has been discussed recently by Glicksman *et al.*[7,8]. The interactions among particles and the fluctuations in their individual growth rates induced by their "locale" are complicated influences, so it is not surprising that it is difficult to treat stochastics either analytically or experimentally. It is for this reason that to gain even limited heuristic insight into the stochastics of microstructures, large-scale simulations must play a central role. The earliest study of multiparticle phenomena in micorstructures was published in 1973 by Weins and Cahn[9], who used a few particles to simulate some basic coarsening interactions during sintering. Their study was followed by Voorhees and Glicksman[10] who systematically studied the behavior of several hundred particles randomly placed in a periodic, three-dimensional, unit cell to simulate coarsening. Later, Beenaker[11] further improved multiparticle simulation procedures and was able to increase the total number of particles during simulation. More recently, other investigators[8,12-15], continued to improve the accuracy of large-scale simulation of microstructural coarsening processes. Studying the interactions among many particles and including the statistics of their fluctuations during growth and dissolution, even in the case of very small volume fractions, can contribute important facts required in the understanding of real microstructures. In this paper, we shall focus on early progress being made on these issues at our laboratory.

This article is organized as follows: The theories for a finite system with nonzero volume fraction, along with that for an infinite system with zero volume fraction (LSW) are presented in section 2. In section 3, details of the modeling and numerical simulations are given. The results for the observed growth law for particles, their steady-state PSD's, and the characteristics of the statistical fluctuations in individual particle growth rate are presented in section 4. Finally, a few conclusions are presented in the last section.

2. Theoretical Analysis

2.1 Theory for finite microstructures with nonzero volume fraction

One can simulate only finite microstructural systems, due obviously to the finite nature of computing power and memory. A theoretical approach to treat a finite system comprises the first essential step to improve the extent and accuracy of numerical simulations. We proceed with an analysis of a system consisting of a large but finite number of polydisperse spherical precipitate particles suspended throughout the volume of a three-dimensional, isotropic matrix phase. Although we begin this analysis with a set of microstructural definitions more aptly applied to an *infinite* system, eventually we restrict and apply the mathematical results to *finite* microstructures. The sizes of the domains comprising the population of dispersed particles are described with a distribution function, $F(R, t)$, defined here conventionally as the number of particles per unit volume at time t, with radii in the range R to $R + dR$. The normalization for $F(R, t)$ is based on the total number of particles per unit volume, N_v, that is,

$$\int_0^\infty F(R, t)dR = N_V, \tag{1}$$

where N_v is the number density of spherical particles. With this normalization the corresponding volume fraction, V_v, of the dispersed phase (total volume of dispersoid per unit volume of the microstructure) is defined consistently as

$$V_V \equiv \frac{4\pi}{3}\int_0^\infty R^3 F(R,t)dR. \tag{2}$$

Equation 2 may be rewritten as

$$V_V = \frac{4\pi}{3} N_V < R^3 >, \tag{3}$$

where $<R^3>$ represents the average of the cube of the particle radii, R.

The biphase microstructure under consideration is aged sufficiently so that the supersaturation of the matrix solution may be assumed to small. Thus, it follows, that nucleation of new particles within the aged microstructure is precluded. This condition constitutes the chief thermodynamic requirement for "late-stage" phase coarsening.

The continuity equation for smoothly growing and dissolving dispersed particles in size space is

$$\frac{\partial F(R,t)}{\partial t} + \frac{\partial}{\partial R}[v(R)F(R,t)] = 0. \tag{4}$$

Here *v(R)* is the time-rate of change of the radius, *R,* of a particle. Equation 4 precludes "non-smooth" changes in the microstructure such as nucleation, particle splitting, and agglomeration, To obtain *v(R),* some additional simplifying assumptions are needed: (1) the kinetics of coarsening is determined by volume diffusion through the matrix; and (2) the diffusion transport to or from each particle occurs slowly enough to be considered quasi-static. These additional assumptions justify approximating the diffusion equation with Laplace's equation to describe the concentration fields, *C(**r**),* in the matrix. Thus, the diffusion field surrounding a particle may be described by

$$\nabla^2 \mathrm{C}(\boldsymbol{r}) = 0, \tag{5}$$

where $\mathrm{C}(\boldsymbol{r}) = (\mathrm{c}(\boldsymbol{r}) - \mathrm{c}_0)/\mathrm{c}_0$ defines a dimensionless diffusion potential, $\mathrm{c}(\boldsymbol{r})$ is the concentration at any point defined by the position vector, $\boldsymbol{r}$, and c_0 denotes the equilibrium solubility at a flat interface between the matrix and particle phases.

The boundary conditions at the spherical interface of the i^{th} particle are specified through the Gibbs-Thomson (or Thomson-Freundlich) local equilibrium solubility relation, namely,

$$C(R_i) = l_c / R_i, \tag{6}$$

where l_c is a capillary length, usually of near atomic dimensions, defined by

$$l_c \equiv 2\frac{\gamma\Omega_a}{k_B T}. \tag{7}$$

In Eq. 7, γ denotes the specific interfacial free energy between the particle and matrix, Ω_a is the particle's atomic volume, k_B is Boltzmann's constant, and T is the absolute temperature.

The solution to Laplace's equation for *n* particles (some acting as sources and some as sinks) distributed as a three-dimensional polydispersion throughout the matrix may be represented as the superposition of *n* dimensionless concentration fields summed over the microstructure.

$$\mathrm{C}(\boldsymbol{r}) = \sum_{i=1}^{n} \frac{\mathrm{l_c B}_i}{|\boldsymbol{r} - \boldsymbol{r}_i|} + \mathrm{C}_\infty. \tag{8}$$

The vector $\boldsymbol{r}$ appearing in Eq. 8 is the field point, always located in the matrix, whereas $\boldsymbol{r}_i$ is a vector that locates the center of the i^{th} particle in the microstructure.

The i^{th} particle's volume flux equals $4\pi B_i$, and the far-field potential C_∞, comprise together, for all *n* particles, a total of $n + 1$ unknowns that must be determined in solving Eq. 8 for the microstructure's diffusion field. The far-field potential C_∞ is found by using global mass conservation. The following conservation law may be written for a discrete system consisting of *n* spherical particles each competing for, but also conserving, the solute transported via diffusion through the matrix phase:

$$\sum_{i=1}^{n} B_i = 0. \tag{9}$$

Substituting the expression for the diffusion potential, Eq. 8, along with the mass conservation condition, Eq. 9, one obtains after a few steps of algebra

$$C_\infty = \frac{l_c}{\langle R \rangle} - \frac{l_c}{n\langle R \rangle}\sum_{k=1}^{n} B_k \sum_{j \neq k}^{n} \frac{R_j}{r_{jk}}, \tag{10}$$

where r_{jk} is the distance between the centers of any pair of particles j and *k.* The relationship, Eq. 10, used to define C_∞, is employed to interpret microstructure responses for the first time. Eq. 10 clearly demonstrates that the far-field potential, C_∞, depends explicitly on the size of the microstructural system, i.e. , on the number of particles, *n,* and on local information concerning particle positions and the distances between pairs of them. In fact, Eq. 10 establishes an important bridge between detailed computer simulations carried out for a finite, discrete system of *n* particles, and the averaged behavior predicted for an infinite, continuous

systems. Equation 10, in fact, includes enough detailed environmental information to describe the "locale" of every particle, and, most importantly, its subtle influence on the particle's diffusion-limited growth or shrinkage. The environmental information built into Eq. 10 is normally excluded from mean-field descriptions of microstructure evolution, but if included, adds important microstructural physics to the diffusion solution.

The assumption of describing C(**r**) using a quasistatic (conservative) diffusion field requires that the mass transfer to or from a particle is equal to its change of mass. Thus, using Eq. 8, the time-rate of change of a particle's radius, dR/dt, is directly connected to the volume flux, B_i, as

$$v(R_i) \equiv \frac{dR_i}{dt} = \frac{-2l_c D_0 c_0 \Omega_a B_i}{R_i^2}, \qquad (11)$$

where D_0, appearing on the right-hand side of Eq.(11), is the interdiffusion coefficient for solute in the matrix.

In principle, the volume fluxes, B_i, can be determined by substituting both the Gibbs-Thomson local equilibrium relation, Eq. 6, and the far-field potential, Eq. 10, into Eq. 8. However, one cannot obtain a useful analytical result for a finite system, excepting the limiting case of an infinite system with *zero* volume fraction. We can determine numerically the volume fluxes from Eqs. 6, 8, and 10, and then substitute the values of the B_i' s into the growth rate relationship, Eq. 11. In this manner, one may solve Eq. 11 numerically, and find the so-called "kinetic" equation for particle growth and shrinkage, enabling prediction of the particle size distribution. The details for accomplishing this are provided in the next section.

2.2 Theory for infinite systems with zero volume fraction

If the number of particles comprising a biphase microstructure rises without limit, so $n \to \infty$, but the matrix volume is allowed to increase sufficiently to become diluted to an infinitesimal particle density, so that $V_v \to 0$, (i.e., distances, r_{jk}, between particle pairs increase indefinitely) then Eq. 10 reduces to the limiting form

$$C_\infty = \frac{l_c}{\langle R \rangle}. \qquad (12)$$

Eq. 12 was derived originally by Todes[1] under his assumption of an "infinite system" with *zero* volume fraction of particles. For the case of such an infinite, yet infinitely diluted system, one may substitute Eq. 12 and Eq. 6 into Eq. 8 and show that the volume fluxes per steradian, B_i' s, reduce to the linear form

$$B_i = 1 - \frac{R_i}{\langle R \rangle}. \qquad (13)$$

If it is assumed that $<R> = R^*$, where R^* is the "critical radius" defined later in Lifshitz and Slyozov's paper[2], then Eq. 13 reduces to the usual LSW formulation. Substituting Eq. 13 into Eq. 11, the LSW growth rate for a particle becomes

$$v(R_i) \equiv \frac{dR_i}{dt} = \frac{-2l_c D_0 c_0 V_a}{R_i^2}\left(1 - \frac{R_i}{\langle R \rangle}\right). \qquad (14)$$

Substituting Eq. 14 into Eq. 4, finding the self-similar solution to Eq. 4, and then applying the LSW stability argument based on mass conservation for the particle population that 1 there exists some maximum particle size and 2 that the time rate of change of the maximum sized particle, relative to the growing average, must vanish, yields the (dimensional) growth law of any particle of radius R as

$$\langle R(t) \rangle^3 - \langle R(0) \rangle^3 = \frac{4}{9}(D_0 l_c c_0)t. \qquad (15)$$

Equation 14, which provides the basis for Equation 15, is a deterministic growth rate law, insofar as the rate of growth or shrinkage of every particle is solely a function of its radius. Indeed, in such an infinitely-diluted microstructure, each particle would exist perhaps somewhat illogically-in total isolation from all its "neighbors." LSW theory also predicts that the particle size distribution (PSD) is *affine,* or self-similar. If the particle sizes are expressed as radii normalized to the growing average, or critical, radius, then the affine form of the PSD does not change with time. Self-similarity of coarsening quasi-spherical microstructures has been demonstrated experimentally in Pb-Sn alloys by Hardy and Voorhees[14].

2.3 Microstructural interactions

In order to extend LSW theory to cases of non-zero volume fraction, a number of markedly different approaches were developed. Marqusee and Ross[16] were the first to model the effects of *non-zero* volume fraction on phase coarsening kinetics by using active-medium theory to describe the quasi-static diffusion fields. The emission of solute from dissolving particles, or absorption of solute from growing ones, are modeled by using point sources or sinks of solute distributed within the matrix. Furthermore, those investigators limited the spatial extent of diffusional interactions by allowing "diffusional screening" to occur active-medium approach led to the use of Poisson's equation to replace the Laplace approximation for quasi-static diffusion,

$$\nabla^2 C(\boldsymbol{r}) = -4\pi\sigma, \qquad (16)$$

where the source or sink density, σ, appearing in Eq.(16) is given by

$$\sigma = N_V (l_c - \langle R \rangle C(\boldsymbol{r})). \quad (17)$$

Re-organizing these Eqs. 16 and 17 yields the diffusion analog of the Debye-Hückel equation, namely[13]

$$\nabla^2 C(\boldsymbol{r}) - \kappa^2 (C(\boldsymbol{r}) - C_\infty) = 0, \quad (18)$$

Here $\kappa \equiv (4\pi N_v \langle R \rangle)^{1/2}$ is introduced as the diffusion analog of the reciprocal of the Debye screening length, and $C_\infty = l_c / R^* \approx l_c / \langle R \rangle$ is the far-field diffusion potential. Eq.(18) is well known from theories of ionic solutions and plasmas. In three dimensions, the general solution to the Debye-Hückel equation for diffusion around a spherical source or sink, subject to the Gibbs-Thomson boundary condition, may be expressed in the form of the well-known Yukawa potential. The spherically symmetric diffusion solution being sought may be written in terms of the volume fluxes as

$$C(\boldsymbol{r}) = \sum_{i=1}^{n} l_c \frac{B_i}{|\boldsymbol{r} - \boldsymbol{r_i}|} \exp(-\kappa |\boldsymbol{r} - \boldsymbol{r_i}|) + C_\infty, \quad (19)$$

where now the B_i' s are defined as

$$B_i = (1 - \frac{R_i}{R^*})(1 + \kappa R_i). \quad (20)$$

The diffusion fields obeying Eqs. 19 and 20 surrounding spherical particles embedded in an "active" matrix phase are shown plotted in Fig. 1. For illustrative purposes, the critical particle size, R^*, used in Fig. 1 to normalize all length scales, was chosen to be l_c, so that the mean concentration, or diffusion potential, $C_\infty = 1$. (In reality, dispersoids in aged microstructures usually have critical radii between circa 10^3 l_c to 10^5 l_c, so that our choice of R^*/l_c merely introduces a convenient scale factor of unity into the diffusion potential). In addition, the dispersoid volume fraction is arbitrarily set to be 0.05, which is sufficiently small so that $R^* \approx \langle R \rangle$, but large enough to have interactions occurring among the particles. Note that the fields plotted in Fig. 1 show that the gradients are negative around all particles smaller than the average, i.e., those for which $\rho \leq 1$, and that these gradients increase sharply in magnitude as the particles become smaller and more curved. Also, the gradients adjacent to larger particles-those for which $\rho \geq 1$ -remain relatively small when compared to the gradients around smaller particles. The gradients surrounding "critical" particles are, by definition, zero, because at the instant depicted in Fig. 1, "critical" particles-those for which $\rho = 1$ -are conditionally stable, and would neither be growing nor shrinking. The scheme of *relative* diffusion potentials and their gradients depicted in Fig. 1 makes clear the "competitive" nature of multiparticle diffusion. Specifically, at every instant, small particles (relative to the average-size particle) are forced to shrink rapidly; larger than average-size particles grow at the expense of dissolving smaller particles, and

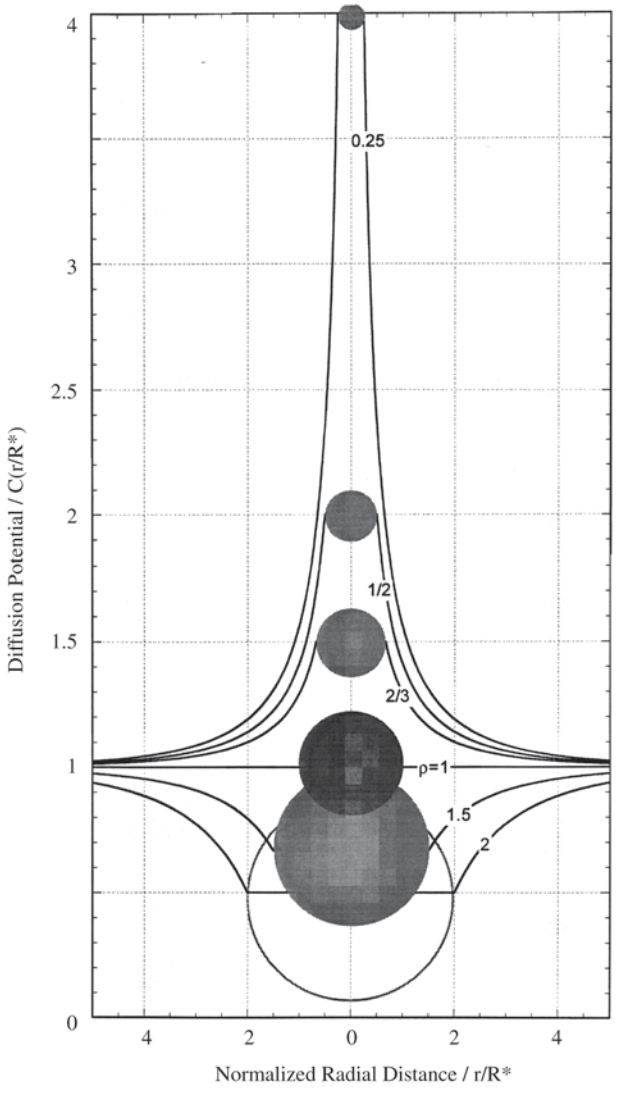

Figure 1. Diffusion fields, $C(\zeta; \rho; V_v)$, based on Debye-Hückel theory during phase coarsening in a microstructure with a dispersoid volume fraction of V_v=0.05. The dimensionless potential plotted here represents the expression for the normalized field, $C(\zeta; \rho; V_v) = (1- \rho) \exp(\rho \sqrt{3}\, V_v)\exp(-\zeta \sqrt{3}\, V_v)/ \zeta + 1$, where $\zeta = r/R^*$ is the running (distance) variable. Each field is labeled by the value of the scaled particle radius, $\rho \equiv R/R^*$, with which it is associated. Note that the field gradients are negative for particles less than critical size ($\rho \leq 1$), and positive for particles greater than critical size ($\rho \geq 1$). The critical sized particle ($\rho = 1$) is shown surrounded by a constant field (zero gradient) at the average diffusion potential, C_∞=1, in the matrix phase.

average-size (critical) particles themselves are conditionally stable and neither grow nor shrink. What makes the overall kinetics of competitive multiparticle aging so interesting is that the average-size particle in the population itself increases with time, in accord with Eq. 15. Thus, the polydisperse population of particles is constantly in "competition" with average-size particles that inexorably grow as the cube-root of time. The net result of this coupled competitive diffusion process is a microstructural population that maintains an affine distribution for all time. That is, the PSD remains identical except for a scale factor that increases as the cube-root of time.

Glicksman, Wang and Marsh[6] recently proved that the diffusional Debye screening length L_D (κ^{-1}), which effectively limits the distance over which the diffusion potential of one particle affects another, is related to the ratio of moments of the PSD and to the reciprocal square-root of the volume fraction of the system,

$$L_D = \sqrt{\frac{\langle R^3 \rangle}{3\langle R \rangle V_V}}. \qquad (21)$$

Equation 21, in fact, can be employed to gauge the interaction length scale in a three-dimensional microstructure undergoing diffusion-limited coarsening, and compare the results with computer simulation or experiment. Moreover, as indicated in Eq. 21, the volume fraction of the microstructure, V_v, is the main factor that acts to reduce the Debye screening length. The population of dissolving and growing particles collectively act to "cuts off" the diffusion field emanating from each particle beyond the Debye screening distance, L_D. This interesting screening effect is shown in Fig. 2, where the diffusion potentials for a small particle ($\rho \leq 1$), a critical particle ($\rho = 1$) , and a large particle ($\rho \geq 1$) are plotted for several values of the volume fraction. A volume fraction of *zero* denotes the behavior expected in the LSW model, where the screening distance becomes infinite, and the Yukawa potential reduces to the Laplace potential. At *non-zero* volume fractions, the gradients steepen, especially around larger particles, and the diffusion fields drop off to the mean potential ($C_\infty = 1$) much faster than for the limiting *case* where $V_v = 0$. Thus, Debye screening tends to speed up diffusive transport in a microstructure, and increases the kinetics of phase coarsening.

3. Modeling and Simulation of Microstructures

3.1 Modeling

The microstructure is modeled by placing *n* particles of the dispersoid phase in a cubic box. The contiguous spaces between the particles represents the matrix phase in which the dispersoid population is embedded. Particles are located by specifying the positions of their centers with three random coordinates representing the Cartesian vector, $\boldsymbol{r}_i$, and by their radii, R_i, chosen initially from a relatively narrow Gaussian distribution. These radii are non-dimensionalized by the capillary length, l_c, a material property based on thermodynamic data, and the microstructure evolution time is non-dimensionalized by a characteristic diffusion time, another property based on the materials transport coefficients, defined as $\tau_d \equiv - l_c^2/(\Omega_a D_0 c_0)$. The dimensionless form of the

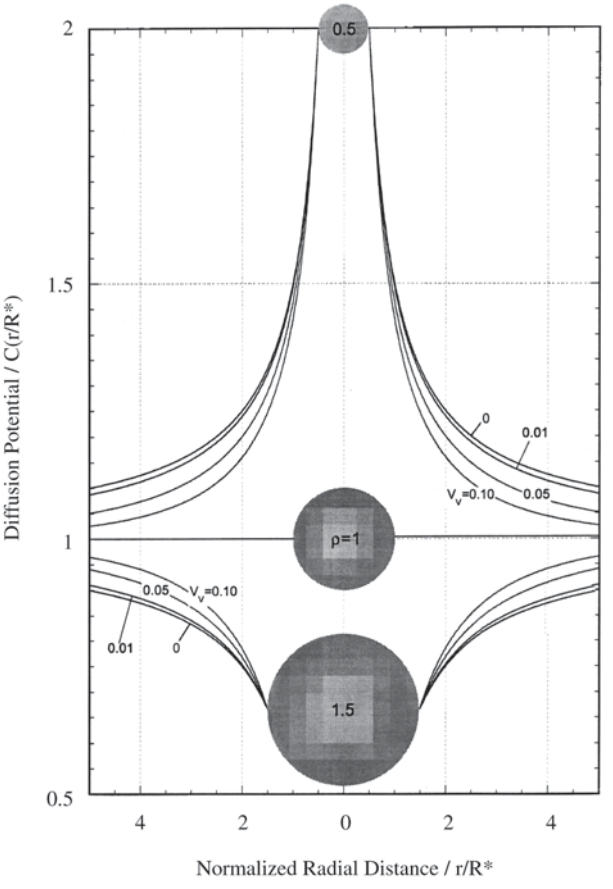

Figure 2. Influence of dispersoid volume fraction, V_V, on diffusion fields. Fields are shown for a small particle ($\rho = 0.5$), a large particle ($\rho = 1.5$), and for the critical particle ($\rho = 1$). The field labeled $V_V = 0$ is that predicted from LSW theory. As V_V increases from zero to represent real biphase microstructures, the diffusion fields decay more rapidly with increasing distance from the particle centers. In addition, increasing the volume fraction steepens the gradients near larger particles, but has a relatively minor influence on the gradients surrounding smaller particles. The Debye screening distance, not shown here, provides a measure of the average field-decay distance for the population of particles comprising the microstructure.

growth rate, Eq. 11, can be written as

$$\frac{dR_i}{dt} = -\frac{B_i}{R_i^2} \qquad (i = 1,2,...n), \tag{22}$$

where R_i is known at the time t. Assuming that all the B_i's are known, numerical integration of the growth rate, Eq. 22, can be used in a forward marching scheme to evolve the radii. The Runge-Kutta technique, was used to evaluate $R_i(t + \Delta t)$. Here, Δt represents each subsequent time step in the marching integral. One, of course, must re-determine the volume fluxes, B_i at each subsequent time step.

Introducing Eq. 8 into Eq. 6, along with the non-dimensionalized system of linear equations, one may cast these equations into matrix form as follows:

$$\boldsymbol{A} \bullet \boldsymbol{B} = \boldsymbol{U}, \tag{23}$$

where A is the $(n + 1)$ by $(n + 1)$ matrix

$$\mathbf{A} = \begin{bmatrix} 1/R_1 & 1/r_{12} & 1/r_{13} & \cdots & 1/r_{1n} & 1 \\ 1/r_{21} & 1/R_2 & 1/r_{23} & \cdots & 1/r_{2n} & 1 \\ 1/r_{31} & 1/r_{32} & 1/R_3 & \cdots & 1/r_{3n} & 1 \\ \vdots & \vdots & \vdots & \cdots & \vdots & \vdots \\ 1/r_{n1} & 1/r_{n2} & 1/r_{n3} & \cdots & 1/R_n & 1 \\ 1 & 1 & 1 & \cdots & 1 & 0 \end{bmatrix}, \tag{24}$$

and where r_{ij} represents the separation between a pair of particles i and j. B and U are $(n + 1)$ by 1 column matrices, namely,

$$\mathbf{B} = \begin{bmatrix} B_1 \\ B_2 \\ B_3 \\ \vdots \\ B_n \\ C_\infty \end{bmatrix}, \tag{25}$$

and

$$\mathbf{U} = \begin{bmatrix} 1/R_1 \\ 1/R_2 \\ 1/R_3 \\ \vdots \\ 1/R_n \\ 0 \end{bmatrix}. \tag{26}$$

Equation 23 represents $(n + 1)$ linear equations. Substituting Eq. 10 into Eq. 23 and eliminating the $(n + 1)^{th}$ row and column in matrix A, allows reduction of Eq. 23 to n linear equations, which may be written as the matrix equation

$$\mathbf{A}' \bullet \mathbf{B}' = \mathbf{U}', \tag{27}$$

where A' is the n by n matrix

$$\mathbf{A}' = \begin{bmatrix} \frac{1}{R_1} - \frac{1}{n\langle R\rangle}\sum_{j\neq 1}^{n}\frac{R_j}{r_{j1}} & \frac{1}{r_{12}} - \frac{1}{n\langle R\rangle}\sum_{j\neq 2}^{n}\frac{R_j}{r_{j2}} & \cdots & \frac{1}{r_{1n}} - \frac{1}{n\langle R\rangle}\sum_{j\neq n}^{n}\frac{R_j}{r_{jn}} \\ \frac{1}{r_{21}} - \frac{1}{n\langle R\rangle}\sum_{j\neq 1}^{n}\frac{R_j}{r_{j1}} & \frac{1}{R_2} - \frac{1}{n\langle R\rangle}\sum_{j\neq 2}^{n}\frac{R_j}{r_{j2}} & \cdots & \frac{1}{r_{2n}} - \frac{1}{n\langle R\rangle}\sum_{j\neq n}^{n}\frac{R_j}{r_{jn}} \\ \vdots & \vdots & \cdots & \vdots \\ \frac{1}{r_{n1}} - \frac{1}{n\langle R\rangle}\sum_{j\neq 1}^{n}\frac{R_j}{r_{j1}} & \frac{1}{r_{n2}} - \frac{1}{n\langle R\rangle}\sum_{j\neq 1}^{n}\frac{R_j}{r_{j2}} & \cdots & \frac{1}{R_n} - \frac{1}{n\langle R\rangle}\sum_{j\neq n}^{n}\frac{R_j}{r_{jn}} \end{bmatrix} \tag{28}$$

$$\mathbf{B}' = \begin{bmatrix} B_1 \\ B_2 \\ \vdots \\ B_n \end{bmatrix}, \tag{29}$$

and

$$\mathbf{U}' = \begin{bmatrix} \frac{1}{R_1} - \frac{1}{\langle R\rangle} \\ \frac{1}{R_2} - \frac{1}{\langle R\rangle} \\ \vdots \\ \frac{1}{R_n} - \frac{1}{\langle R\rangle} \end{bmatrix}. \tag{30}$$

The Gauss-Seidel method was employed to solve this system of linear equations, Eq. 27, yielding at each time step values for the B_i's. Substitution of the up-dated B_i's back into Eq. 22 dynamically advances the microstructure by up-dating the radii of all the particles and their coordinates at any time step.

3.2 Simulation of microstructures

As described briefly above, the simulation of the evolving microstructure is initiated by defining an assembly of n

particles obeying some initially chosen size distribution. These initial particles are placed randomly within a cubic box to comprise the initial microstructure. The box size may be determined from the specified volume fraction, V_v, the initial number of particles, *n(0),* and their starting distribution.

The choice of time-step in performing the integration of Eq. 22, is crucial. Large time-steps that allow the system to evolve quickly do not permit sufficiently accurate solutions to the microstructure evolution equation, Eq. 22. Too large a time step may result in an unsatisfactory PSD. At each time step, the computational program checks the radius of every particle. If any became smaller than $0.1l<R>$, they are removed from the simulation box and considered "dissolved". Equivalently, the column and row corresponding to a dissolved particle is struck from the matrix, Eq. 28. The initial number of particles forming the microstructure influences the total run time. Specifically, data are collected from each simulation throughout the time period for which mass is conserved and the volume fraction remains constant to within a prescribed tolerance. It is observed, not surprisingly, that the greater the number of particles forming the initial microstructure, the better is the accuracy of the simulation, the longer the run may be evolved, and the faster the statistics for the data settle to steady trends. However, numerical difficulties are eventually encountered as the number of particles, *n,* and thus the number of linear equations**,** n^2, increase. The larger the number of particles, the greater is the required computer memory, and the longer is the CPU time required to evolve the system. Ultimately, the increasing CPU time limits the practicality of these simulations for large microstructural assemblages.

4. Results

Simulation of microstructural coarsening was carried out for volume fractions covering the range $10^{-4} < V_v < 10^{-1}$. Figure 3 shows that for values of the time, *t,* larger than about 0.3, the cube of the average radius of the particles increases linearly with time. The "cube-root of time" kinetics, is a well-known prediction from LSW theory for diffusion-limited coarsening, and is confirmed by numerous experiments. Figure 4 displays the PSD developed in the simulated microstructure. The radii plotted here are scaled by the average radius of the particle population for a volume

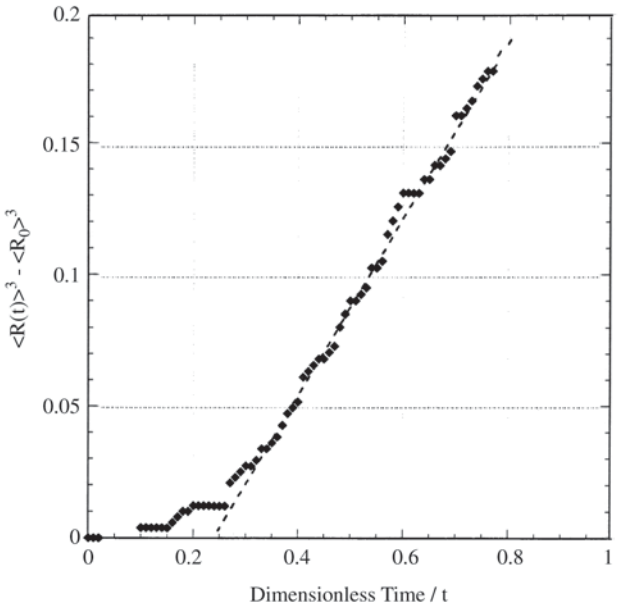

Figure 3. Average of the radius of the particle population cubed, versus time. The predicted linearity of $<R>^3$ against time develops only after the PSD develops its affine form. Before becoming affine, or "self-similar," the PSD evolves through the transient evolution of the microstructure's dispersoid population. Dashed line provided only as a guide to judge the achievement of the predicted linear behavior.

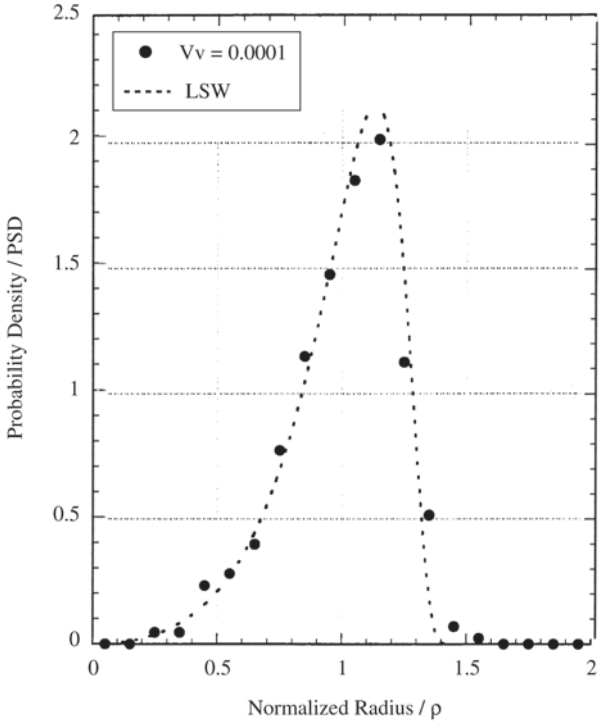

Figure 4. Particle size distribution (PSD). Plot of the probability density, G(ρ), of finding particles of radius ñ in a small range of sizes, dρ, versus normalized particle radius. Data are for a small but *non-zero* volume fraction ($V_V = 10^{-4}$). At finite, *non-zero* values of V_V, the PSD broadens toward larger *radii*, drops in height, and becomes slightly more symmetrical than predicted from LSW theory. Multiparticle interactions are responsible for these changes.

fraction of $V_v = 10^{-4}$. The PSD predicted from LSW theory ($V_v = 0$) is shown in Fig. 4 for comparison. Neither prior theoretical, experimental, nor simulation results are available for $V_v = 10^{-4}$. Figure 4 clearly indicates that microstructures with even a small volume fraction of particles exhibit detectable broadening of the PSD and a marked decrease its peak height**,** as compared with that predicted from LSW theory.

Figure 5 displays the form of the computed volume fluxes, B(ρ) for *zero* volume fraction and for $V_v = 10^{-4}$. LSW theory predicts that the volume flux has a linear variation with the scaled particle radius, that is, $B(\rho) = 1 - \rho$. However, as is also indicated in Fig. 5, the simulation for $V_v = 10^{-4}$ shows clearly that particles of identical size actually exhibit a small range of flux values scattered around the LSW prediction. The growth rate experienced by a particle of radius ρ, even at a relatively small volume fraction, is not a purely deterministic quantity as predicted by mean-field theory.

Figures 6 through 8, show the volume fluxes B(ρ) simulated for $V_v = 10^{-3}$, $V_v = 10^{-2}$, and 10^{-1}, respectively. These figures demonstrate that the B(ρ)'s steadily deviate from the linear LSW prediction. It is also evident from these

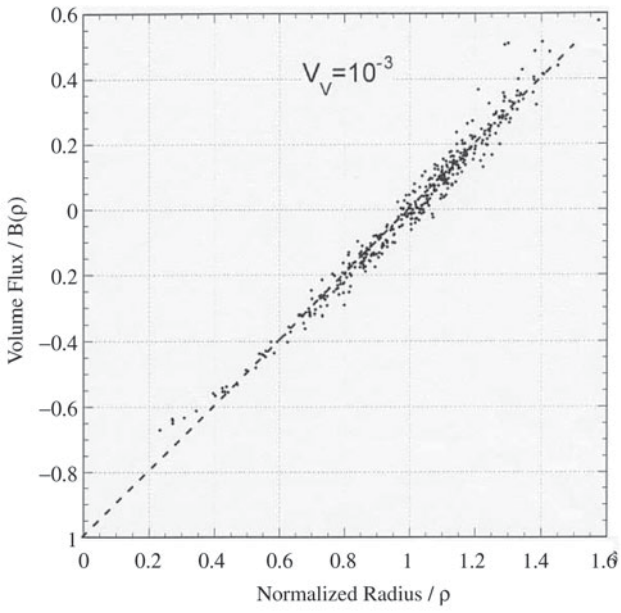

Figure 6. Volume flux per steradian, B(ρ), versus scaled particle radius, ρ. Data are simulated from the multiparticle diffusion model for a microstructure with a dispersoid volume fraction $V_V = 10^{-3}$. Note the broadened noise band as compared to that in Fig. 5.

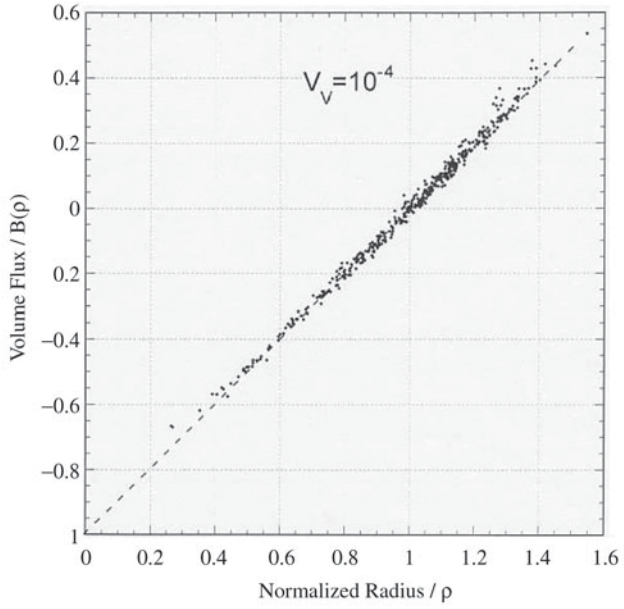

Figure 5. Volume flux per steradian, B(ρ), versus scaled particle radius, ρ. Data are simulated from the multiparticle diffusion model for a microstructure with a dispersoid volume fraction $V_V = 10^{-4}$. The associated microstructural noise distribution for these fluxes is shown by the scatter of the simulation data relative to the noise-free linear flux function (dashed line) predicted from LSW theory. Even at this small (but *non-zero*) volume fraction, discernible fluctuations, or "locale noise", are evident.

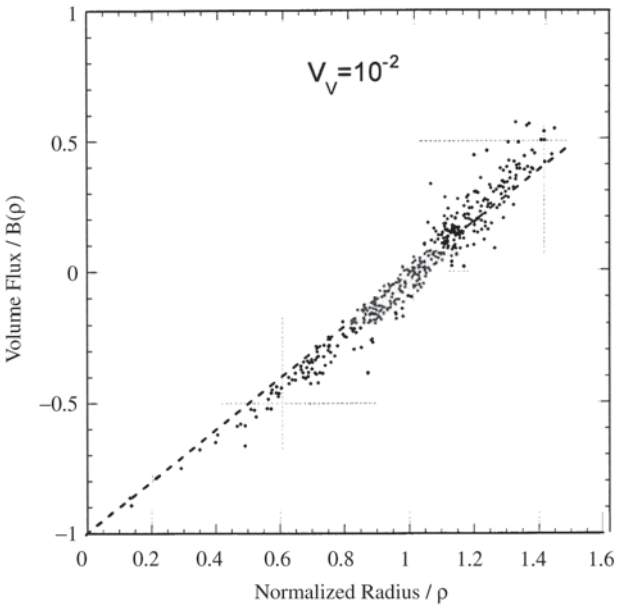

Figure 7. Volume flux per steradian, B(ρ), versus scaled particle radius, ρ. Data are simulated from the multiparticle diffusion model for a microstructure with a dispersoid volume fraction $V_V = 10^{-2}$. Note that the noise band continues to broaden when compared to the simulation data shown in Fig. 6, and that the fluctuations are noticeably asymmetrical with respect to the linear LSW prediction (dashed line). Broadening of locale noise is especially evident for larger particles.

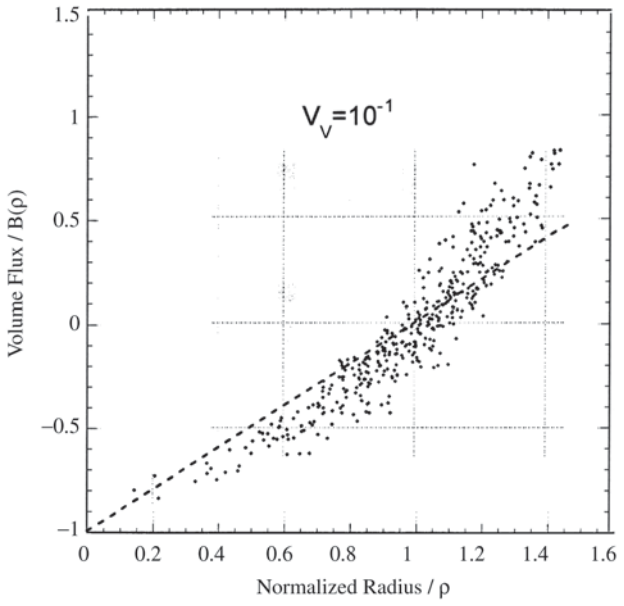

Figure 8. Volume flux per steradian, B(ρ), versus scaled particle radius, ρ. Data are simulated from the multiparticle diffusion model for a microstructure with a dispersoid volume fraction $V_V = 10^{-1}$. Locale noise, except perhaps for the smallest particles exhibits strong stochastic behavior. That is, particles, particularly those close to the average size within the simulated microstructure, act unpredictably by occasionally growing or dissolving rapidly. Were the average size particles to act deterministically, they would hardly grow or shrink at all. The fluctuations at this volume fraction also exhibit non-linear departures from the LSW prediction (dashed line).

simulations that the fluctuation, or "noise" band for the volume fluxes increases with increasing volume fraction.

5. Conclusions

Microstructure evolution in a two-phase system was simulated by solving a large linear matrix equation that describes multiparticle diffusion. Particles interacted in the simulated microstructure under conditions close to steady-state, or affine, coarsening. The far-field diffusion potential used in these simulations is derived here for a finite system [c.f. Eq. 10] in this paper. The effects of system size and microstructure locale information for each particle were included in the far-field diffusion potential. As the volume fraction becomes small, our results approach those of Todes[1] and LSW[2,3], exclusive of the weak interactions that persist among particles.

Simulations of diffusion-limited coarsening carried out on sparse to moderately dense microstructures ($10^{-4} \leq V_v \leq 10^{-1}$) display classical coarsening kinetics that is the cube of the average radius increases linearly with time. However, the PSD computed for a biphase microstructure as sparse as $V_v = 10^{-4}$ remains somewhat broader and more symmetric than that predicted by LSW. This is the first PSD derived using simulation at such a small volume fraction.

Mean-field theory treats the growth rates of particles as a deterministic kinetic process that depends only on the size of a particle relative to the average size of the entire microstructural population. In addition, mean-field theories ignore environmental information for individual particles. From the simulations reported here, however, we find that the fluctuation band for a particle's volume flux widens with the increase of volume fraction. Larger particles experience stronger fluctuations, or locale noise, in their growth rates than do smaller particles. The non-linear character of the particle volume flux versus particle size increases steadily with increasing volume fraction. Finally, this work suggests that stochastic effects must always be present in real biphase microstructures and may play an important role in microstructure evolution. Once the statistical nature of microstructural fluctuations are understood, then theories of microstructure evolution can be modified to include their effect. The authors hope that this work will stimulate quantitative experiments that focus on systems at small volume fraction, to help achieve firmer understanding of multiparticle interactions within evolving biphase microstructures.

Acknowledgements

The authors are pleased to acknowledge partial financial support received from the National Aeronautics and Space Administration, Marshall Space Flight Center, Huntsville, AL, under Grant NAG-8-1468.

References

1. Todes, O.M. *J. Phys. Chem. (Sov.)*, v. 20, p. 629, 1946.
2. Lifshitz, I.M.; Slyozov, V.V. "The Kinetics of Precipitation from Supersaturated Solid Solution," *J. Phys. Chem. Solids*, v. 19, p. 35-50, 1961.
3. Wagner, C. "Theorie der Alterrung von Niederschlagen durch Umlosen," *Z. Elektrochem.*, v. 65, p. 581-591, 1961.
4. Alkemper, J.; Snyder, V.A.; Akaiwa, N.; Voorhees, P.W. "Dynamics of Late-Stage Phase Separation: A Test of Theory," *Phys. Rev. Lett.*, v. 82, p. 2725-2728, 1999.
5 Voorhees, P.W. "Ostwald Ripening of Two-Phase Mixtures," *Ann. Rev. Mater. Sci.*, v. 22, p. 197-215, 1992.
6. Glicksman, M.E.; Wang, K.G.; Marsh, S.P. "Diffusional Interactions among Crystallites," *J. Crystal Growth*, v. 230, p. 318-327, 2001.
7. Marsh, S.P.; Glicksman, M.E. "Environmental Noise Effects in Statistical Coarsening Theory," Solidification, ed.

W.H. Hofmeister, J.R. Rogers, N.B. Singh, S.P. Marsh, P.W. Voorhees, The Minerals, Metals & Materials Society, p.229-238, 1999.

8. Glicksman, M.E.; Wang, K.G.; Crawford, P. "Simulations of Microstructural Evolution,"Computational Modeling of Materials, Minerals and Metals Processing, ed. Mark Cross, The Minerals, Metals & Materials Society, p. 703-713, 2001.
9. Weins, J.; Cahn, J.W. "The Effect of Size and Distribution of Second Phase Particles and Voids on Sintering,"Sintering and Related Phenomena, ed. G.C. Kuczynski, Plenum, New York, p. 151-163, 1973.
10. Voorhees, P.W.; Glicksman, M.E. "Solution to The Multi-Particle Diffusion Problem with Applications to Ostwald Ripening-II. Computer Simulations," *Acta Metall.*, v. 32, p. 2013-2030, 1984.
11. Beenakker, C.W.J. "Numerical Simulation of Diffusion-Controlled Droplet Growth: Dynamical Correlation Effects," Phys. Rev. A, v. 33, p. 4482-44835, 1986.
12. Akaiwa, N.; Voorhees, P.W. "Late-Stage Phase Separation: Dynamics, Spatial Correlations, and Structure Functions," *Phys. Rev. E*, v. 49, p. 3860-3880, 1994.
13. Fradkov, V.E.; Glicksman, M.E.; Marsh, S.P. "Coarsening Kinetics in Finite Clusters," *Phys. Rev. E*, v. 53**,** p. 3925-3932, 1996.
14. Hardy, S.C.; Voorhees, P.W. "Ostwald Ripening in a System with a High Volume Fraction of Coarsening Phase." *Metall. Trans. A*, v. 19, p. 2713, 1988.
15. Mandyam, H. *et al*. "Statistical Simulations of Diffusional Coarsening in Finite Clusters," *Phys. Rev. E*, v. 58, p. 2119-2130, 1998.
16. Marqusee, J.A.; Ross, J. "Theory of Ostwald Ripening: Competitive Growth and its Dependence on Volume Fraction," *J. Chem. Phys.*, v. 80, p. 536-543, 1984.